Magnetic dichroism in darkfield UV photoemission electron microscopy

M. Paleschke, D. Huber, J. Henk, and W. Widdra[*]

Institute of Physics, Martin Luther University Halle-Wittenberg, D-06099 Halle (Saale), Germany

F. O. Schumann

Max-Planck-Institut für Mikrostrukturphysik, Weinberg 2, 06120 Halle, Germany

C.-T. Chiang

Institute of Atomic and Molecular Sciences, Academia Sinica, Taipei, Taiwan
(Dated: May 24, 2024)

Here comes the abstract . . .

Introduction. Ultrafast spin and magnetization dynamics are exciting and rapidly growing fields in condensed matter physics, with promising implications for both future research and device applications. Ultrafast imaging of magnetic domains on the micrometer scale is well established based on all-optical methods, as e.g. Kerr microscopy. On the nanometer scale, however, electron microscopy is applied due to the shorted electron de Broglie wavelength. Imaging of magnetic domains typically utilizes magnetic circular dichroism (MCD) analyzed by photoelectron emission microscopy (PEEM). The intensity recorded for a particular domain changes with the helicity of the incident radiation, thereby producing magnetic contrast without the need for an explicit electron spin detection. By tuning the incident light to a magnetic core level absorption edge, substantial and element-specific MCD asymmetries have been reported. With the availability of tunable synchrotron radiation, XMCD-PEEM has matured into a widely used technique for magnetic domain imaging on the nanometer scale and for slow dynamics. However for ultrafast dynamics, the pulse length of synchrotron radiation, which is typically around 30-50 ps, renders XMCD-PEEM unsuitable. Replacing the incident X-ray radiation by ultrashort laser pulses solves this issue straightforwardly and allows for pump-probe experiments on a few femtoseconds timescale. In addition, experiments can be performed in the laboratory.

Determined by the laser photon energy, photoelectrons are excited from the valence band to energies slightly above the escape threshold (i.e., a few tenths of an electronvolt above the vacuum level).

Respective experiments on Ni/Cu(001) with threshold PEEM revealed that the magnetic contrast is very small

Give number

and therefore might not be sufficient for ultrafast imaging

Add reference

. The above calls for improving threshold-PEEM while keeping the advantages of a laser-based experiment. In this paper we report on such a refinement of threshold
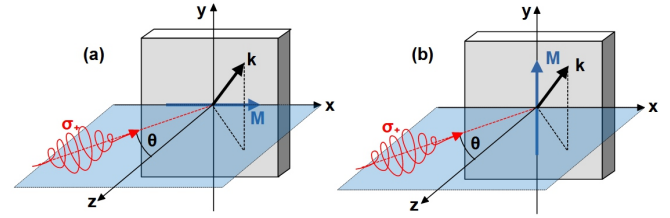

FIG. 1. Symmetry analysis. A circular polarized laser pulse (orange, with helicity σ_+ impinges onto a magnetic domain (rectangular solid, with magnetization direction $\boldsymbol{M}$). The pulse's incidence direction and the surface normal (z-axis) span the scattering plane (blue; xz-plane). The off-normal detection of photoelectrons with wavevector $\boldsymbol{k}$ results in a chiral setup. If the scattering plane is a mirror plane of the latiice, the photoemission intensities for fixed $\boldsymbol{k}$ obey $I(\sigma_+, +\boldsymbol{M}) = I(\sigma_-, -\boldsymbol{M})$ (panel a) or $I(\sigma_+, +\boldsymbol{M}) = I(\sigma_-, +\boldsymbol{M})$ (panel b).

PEEM, in which the magnetic contrast is significantly enhanced. The main idea is to utilize darkfield MCD in threshold photoemission. Momentum and energy selection . . .

We apply the new approach to magnetic domains of Fe(100). It is rationalized by symmetry considerations, and the experimental results are supported by state-of-the-art photoemission calculations. In our opinion, this approach is an essential step toward ultrafast imaging of magnetic domains.

Conceptual basis. Key to the proposed approach are asymmetries of the photoemission intensities, which follow from symmetry consideration. Since a PEEM detects photoelectrons with (almost) all emission angles, one is concerned with a chiral geometry for photoelectrons with off-normal wavevector $\boldsymbol{k}$ (Fig. 1). This chirality results in magnetic dichroism and, hence, in magnetic contrast.

The photoemission intensity of electrons detected with wavevector $\boldsymbol{k}$ depends on the two helicities $\sigma_\pm$ of the incident circular polarized laser radiation and on the two orientations $\pm M$ of the in-plane magnetization in a selected domain, yielding four intensities $I_{\boldsymbol{k}}(\sigma_\pm, \pm M)$ (shortened $I_{\pm\pm}$). The latter are combined into the total intensity

$$I \equiv I_{++} + I_{+-} + I_{-+} + I_{--}. \tag{1}$$

In order to disentangle the two main contrast mechanisms we define appropriate asymmetries:

$$A_{\text{pol}} \equiv \left[(I_{++} + I_{+-}) - (I_{-+} + I_{--}) \right] / I, \qquad (2a)$$

$$A_{\text{ex}} \equiv \left[(I_{++} + I_{--}) - (I_{+-} + I_{-+}) \right] / I. \qquad (2b)$$

In the polarization asymmetry A_{pol} the magnetization's orientation is averaged out; it thus encodes contrast due to the light's helicity (as if the domain were nonmagnetic). Contrast due to the exchange splitting is quantified by the exchange asymmetry A_{ex}, in which one averages over the mutual orientations of helicity and magnetization.

Experimental aspects. Setup ...

The experimental results as well the conceptual ideas are supported by relativistic photoemission computations, briefly described in the Supplemental Material [1].

Contrast mechanisms. In a first step we analyze the two main contrast mechanism: light polarization and exchange splitting.

The polarization asymmetry A_{pol}, defined in Eq. (2a) and depicted in Fig. 2, depends on the binding energy of the initial states. Both theoretical (top row) and experimental data (bottom row) show that this contrast mechanism is sizable (with absolute values up to about 40 % in theory and 20 % in experiment) and thus cannot be ignored.

The theoretical patterns (top row in Fig. 2) exhibit two nodal lines ($k_x = 0$ and $k_y = 0$). Moreover, one finds changes of sign if either k_x or k_y is reversed. These features are imposed by the symmetry of the setup. The experimental counterparts (bottom row) display the same features but slightly oblique or off-center, most clearly for binding energies with comparably small asymmetry (cf. 0.15 eV and 0.25 eV). We attribute these deviations to imperfections in experiment, for example a small misalignment of the light incidence with respect to a crystal mirror plane and inhomogeneous magnetization in the surface layers. Moreover, we assume an electron self-energy that is independent of $k_\parallel$ (see [1]). Nevertheless, the agreement of experiment and theory shows that ...

> More here

The energy-dependent exchange asymmetry A_{ex}, defined in Eq. (2b) and shown in Fig. 3, is smaller than A_{pol} (Fig. 2) (with absolute values up to 10 % in theory and 6 % in experiment). Nevertheless it exhibits a clear odd symmetry upon reversal of k_x; it does not change sign upon reversal of k_y, in contrast to A_{pol}. Both features are dictated by the symmetry of the setup (see [1]).

The above findings support that the asymmetries A_{pol} and A_{ex} are suitable tools to disentangle and to quantify the main contrast mechanisms for domain imaging.

Domain imaging. Aperture, selection of wave vectors.

Center position of the aperture shows very weak contrast (Fig. 4).

Sizable contrast in the other off-center positions of the aperture. Allows to image domain structure unequivocally. Size of contrast/asymmetry ...

Prospects. The present investigation proves that magnetic domains can be imaged with a laser-equipped photoelectron emission microscope with high contrast using a momentum-selection of the detected photoelectrons. The common belief that a such PEEM provides only weak contrast is thereby refuted.

For a proof of principle we applied the proposed improvement to in-plane magnetized Fe(001) surfaces. However, the approach is general so that it can easily be applied to other ferromagnets, even to those with out-of-plane magnetization. Thus, it well suited for studying magnetic reorientation transitions, as for example observed for Ni/Cu(001) . We see its main capabilities in investigations of ultrafast magnetization dynamics using femtosecond laser pulses. As applications one might think of ultrafast motion of domain walls or of large skyrmions.

> Add reference

> Mention racetrack?

[1] See Supplemental Material at [URL will be inserted by publisher] for supporting information and additional results.
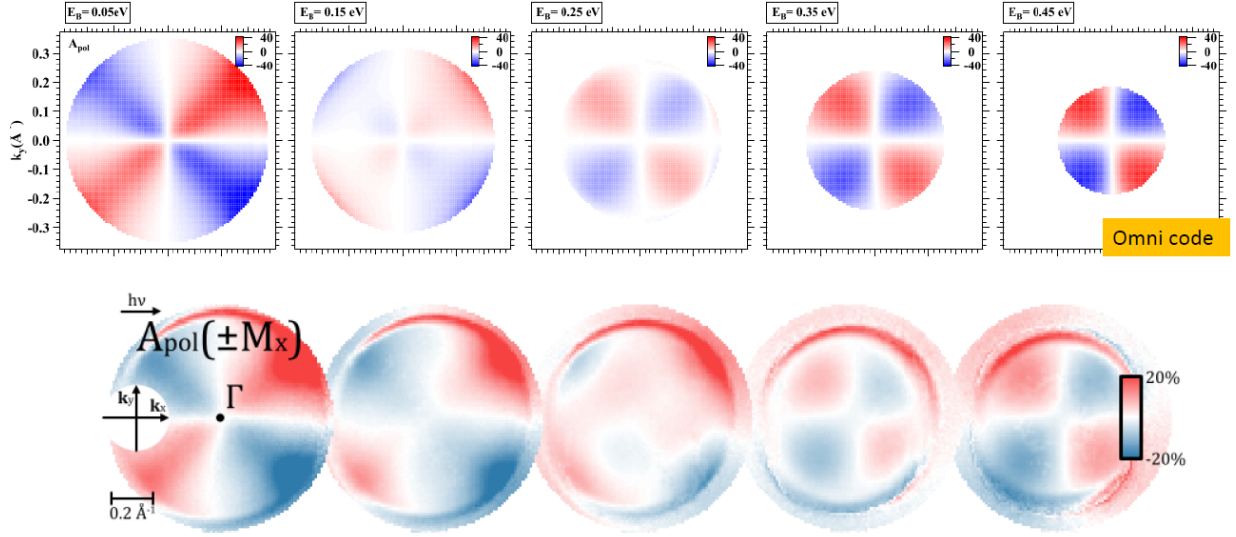
TODO LIST

FIG. 2. Polarization asymmetry A_{pol} of Fe(001) at selected binding energies versus wave vector $\boldsymbol{k}_{\parallel}$ of the photoelectrons. Top row: theoretical results obtained from photoemission calculations. The binding energy is indicated at each panel. The color scale, showing A_{pol} as defined in Eq. (2a) in percent, is identical for all panels in this row. Bottom row: respective experimental results. The arrow marked $h\nu$ indicates the light incidence direction. Γ is the center of the surface Brillouin zone ($\boldsymbol{k}_{\parallel} =$).
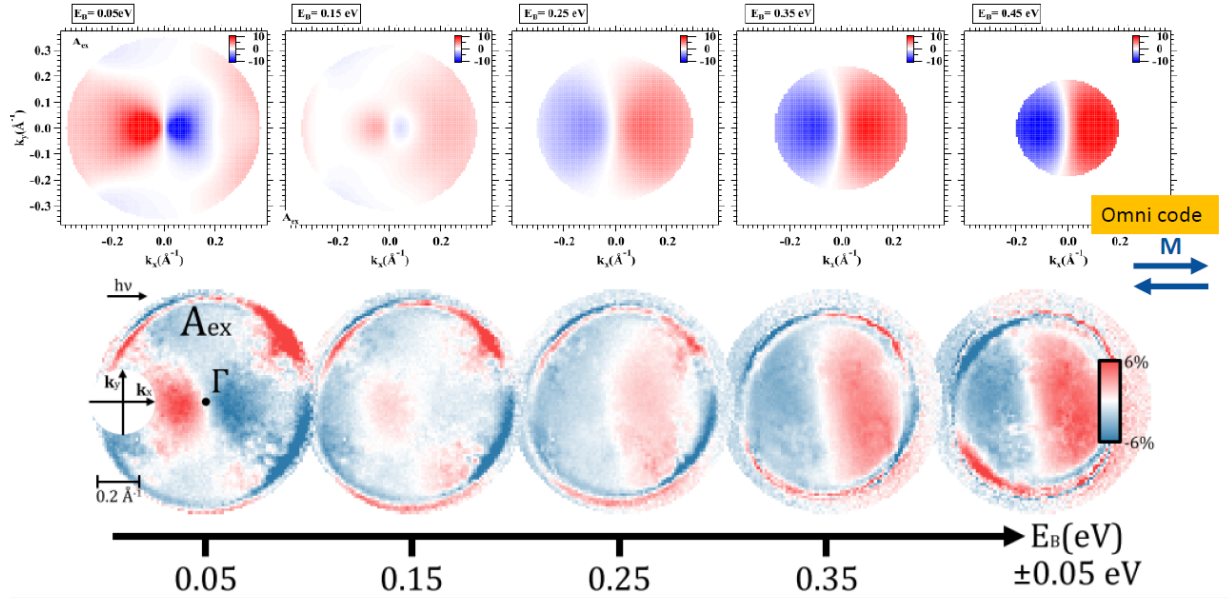

FIG. 3. As Figure 2, but for the exchange asymmetry A_{ex} of Fe(001). The orientations of the magnetization are indicated by arrows on the right-hand side.

FIG. 4. Darkfield magnetic-circular dichroism imaging of Fe(100). Left: schematic, nine aperture positions .... Right: domain imaging using the nine aperture positions.